

Pressure-driven outflow and magneto-centrifugal wind from a dynamo active disc

Wolfgang Dobler¹, Axel Brandenburg^{1,2}, Anvar Shukurov¹

¹Department of Mathematics, University of Newcastle upon Tyne,
NE1 7RU, England

²Nordita, Blegdamsvej 17,
DK-2100 Copenhagen Ø, Denmark

Abstract. We present a numerical model of an accretion disc with mean-field dynamo action that develops pressure-driven collimated outflow near the rotation axis and a centrifugally driven uncollimated wind in the outer parts. The jet is collimated and confined by the azimuthal magnetic field that is produced by the dynamo in the disc and advected to the disc corona. The jet is hot and dense, but has low angular momentum. We also briefly discuss the possible generation of magnetic fields in a jet by the screw dynamo.

1 Introduction

The importance of magnetic fields for accretion is widely recognized, and the turbulent dynamo is believed to be the main source of magnetic fields in accretion discs (Pudritz, 1981; Stepinski & Levy, 1988; Brandenburg et al., 1995). Likewise, magnetic fields are considered a major factor in launching a wind and collimating it into a jet in young stellar objects and active galactic nuclei; see Königl & Pudritz (1999) for a recent review of stellar outflows. Yet, most MHD models of the formation and collimation of jets rely on an externally imposed poloidal magnetic field and disregard any field produced in the disc. Here we discuss how jets can be launched and collimated in systems where the magnetic field is self-consistently generated in the disc. We use parameters of young stellar objects in our estimates, but the basic physical processes discussed might be operative around black holes as well.

Blandford & Payne (1982) showed how jet flows can be launched and collimated by centrifugal and magnetic forces. This idea has been further developed by Ustyugova et al. (1995), Romanova et al. (1997, 1998), Ouyed, Pudritz & Stone (1997), Ouyed & Pudritz (1997a,b, 1999), who consider a perfectly conducting fluid in the corona of an accretion disc, permeated by an external poloidal magnetic field. The physics of the accretion disc is subsumed into the boundary conditions at the base of the corona: the disc at the boundary is assumed to be in Keplerian rotation, no radial inflow is allowed on that boundary, and the system is driven by matter injection from the disc.

Since any accretion is neglected, these models eventually develop a steady state with a magneto-centrifugal wind collimated by the toroidal magnetic field, which again is produced by the vertical shear in rotation (i. e. $\partial\omega/\partial z$).

In our model, no external magnetic field is assumed. We simulate an accretion disc surrounded by a corona, with magnetic field maintained by dynamo action in the disc, with non-ideal, compressible MHD equations and a prescribed entropy profile. The disc rotates at nearly Keplerian velocity in the gravitational field of a central object. A wind develops that carries toroidal magnetic field into the corona. This field eventually collimates the wind, producing a well collimated outflow aligned with the disc rotation axis.

2 The model

A simple way to implement a dense, relatively cool disc embedded in a rarefied, hot corona, is to prescribe an appropriate distribution $s(\mathbf{x})$ of specific entropy, s being small within the disc and large in the corona.

To make our model as simple as possible, we introduce a mass source in order to balance mass loss through the boundaries of the computational domain, so that the continuity equation takes the form

$$\frac{D\rho}{Dt} = -\rho \operatorname{div} \mathbf{u} + q_\rho, \quad (1)$$

where $D/Dt = \partial/\partial t + (\mathbf{u} \cdot \operatorname{grad})$ and \mathbf{u} is the velocity field. The mass source is localized in the disc and described by $q_\rho = \tau^{-1} \xi(\mathbf{x}) [\rho_{\text{ref}} - \rho]_+$, where τ is a short relaxation time, $[\psi]_+ = (\psi + |\psi|)/2$, and ρ_{ref} is the initial equilibrium distribution.

The profile $\xi(\mathbf{x})$ defines our disc, interpolating smoothly between the value 1 in the midplane of the disc, and 0 throughout the corona. We also use it to prescribe the entropy $s(\mathbf{x})$ such that s is low in the disc and high in the corona, the resulting density contrast being of order 10.

The mass source injects matter at Keplerian velocity \mathbf{u}_K , so the equation of motion in a gravitational potential Φ takes the form

$$\rho \frac{D\mathbf{u}}{Dt} = -\operatorname{grad} p - \rho \operatorname{grad} \Phi + \mathbf{F} + (\mathbf{u}_K - \mathbf{u}) q_\rho, \quad (2)$$

where $\mathbf{F} = \mathbf{j} \times \mathbf{B} + \nabla \cdot \boldsymbol{\sigma}$ is the sum of Lorentz and viscous forces, with $\boldsymbol{\sigma}$ the stress tensor.

We solve the induction equation in terms of the vector potential \mathbf{A} ,

$$\frac{\partial \mathbf{A}}{\partial t} = \mathbf{u} \times \mathbf{B} + \alpha \mathbf{B} - \eta \mu_0 \mathbf{j}, \quad (3)$$

so that $\mathbf{B} = \operatorname{rot} \mathbf{A}$ is the magnetic field and the current density \mathbf{j} is given by $\mu_0 \mathbf{j} = \operatorname{grad} \operatorname{div} \mathbf{A} - \Delta \mathbf{A}$. The term $\alpha \mathbf{B}$ is responsible for mean-field dynamo action, producing a predominantly toroidal magnetic field in the disc.

We adopt cylindrical polar coordinates (r, φ, z) and consider axially symmetric solutions of Eqs. (1)–(3).

length	velocity	column density	time	magnetic field	accretion rate
l	c_{s0}	σ_0	l/c_{s0}	$c_{s0}\sqrt{\mu_0\sigma_0/l}$	$l\sigma_0 c_{s0}$
0.1 AU	100 km/s	10 kg/m ²	1.7 d	3 mT (30 G)	$2\times 10^{-7} M_\odot/\text{yr}$

Tab. 1. The units adopted in our model.

Our α -coefficient is of the form

$$\alpha(r, z) = \alpha_0 \frac{z}{z_0} \frac{\xi(r, z)}{1 + v_A^2/v_{A0}^2}, \quad (4)$$

where $v_A = B/\sqrt{\rho\mu_0}$ is the Alfvén speed and v_{A0} is an effective turbulent velocity in the disc, which can be related to the local sound speed c_s . For the magnetic diffusivity we assume $\eta = \eta_0 + \eta_t \xi(r, z)$, which is a sum of a uniform background value η_0 and a turbulent magnetic diffusivity η_t present in the disc.

Our initial state is a hydrostatic equilibrium that is obtained by integrating the equation of motion from $\mathbf{u} = \mathbf{0}$ at infinity down to the midplane. Everywhere outside the disc, $\mathbf{u} = \mathbf{0}$, while in the disc midplane, where temperature is low, $\mathbf{u} \approx \mathbf{u}_K$.

Dimensionless variables are defined using the units given in Table 1. For our reference model we adopt the following set of parameters: $\alpha_0 = -0.3$, $\eta_t = 10^{-3}$, $\eta_0 = 5 \times 10^{-4}$, $v_{A0} = 3 c_s$, $\tau = 0.1$. The disc, as defined by the profile $\xi(r, z)$, has half-thickness $z_0 = 0.15$ and radius $r_0 = 1.5$. The kinematic viscosity is a function of position; it consists of a background value $\nu = 0.02 U_{\max} \delta x$ — where δx is the grid spacing and $U_{\max} = \max(|\mathbf{u}|, c_s, v_A)$ — and a compression-dependent shock viscosity. We also include artificial mass diffusion to stabilize shocks.

The equations are solved numerically, using a finite-difference scheme on the computational domain $0 \leq r \leq 4$, $|z| \leq 4$ with a grid size of 201×401 points. We apply open boundary conditions at the outer boundaries; furthermore, any inward normal component of the velocity field is suppressed there.

3 Results

Motivated by the results of Brandenburg et al. (1995), we choose α_0 negative in Eq. (4). With the numbers given above, the dynamo is in an α^2 regime at $r \lesssim 1$, whereas an $\alpha\Omega$ -dynamo acts in the outer parts of the disc. The dynamo number $\mathcal{D} = C_\alpha C_\omega \simeq 600 r^{-3/2}$ strongly exceeds the critical value (of order 10 without a wind and with vacuum boundary conditions), and a rough estimate of the local magnetic field growth time τ_m due to dynamo action is $\tau_m \simeq 0.5 r^{3/4}$.

The initial, hydro “static” state is unstable, firstly because accretion flow develops spontaneously due to angular momentum transfer by viscous and magnetic stresses and, secondly, because of the vertical shear in the angular velocity between the disc and the corona (Urpin & Brandenburg, 1998). As a result, meridional circulation develops, which soon transforms into a pressure driven wind.

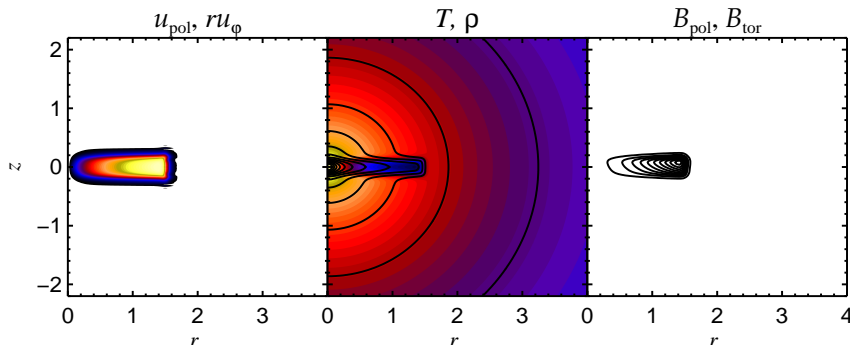


Fig. 1. Initial (hydro“static”) state of the system. Left: initial velocity; ru_ϕ is shown colour coded; \mathbf{u}_{pol} is initially absent. Centre: temperature (colour coded) and density (contour lines). Note the cold, dense disc surrounded by the spherically symmetric corona. Right: magnetic field; B_ϕ is initially absent; field lines of \mathbf{B}_{pol} are shown.

The initial magnetic field differs from zero only in the disc (see Fig. 1) where its strength is 10^{-3} and it is composed of dipolar and quadrupolar components with relative weight 2:1. Without any meridional flows, the dominant mode in a disc with positive \mathcal{D} is an oscillating dipolar mode. The dominant mode becomes steady as soon as significant outflow has developed.

Although the initial magnetic field is poloidal, the dynamo soon amplifies the azimuthal field in the disc, and then supplies it to the corona. As a result, the corona outside the jet region is filled by strong azimuthal field for $t \gtrsim 15$. The main mechanisms producing B_ϕ in the corona are advection by the wind and magnetic buoyancy.

The field in the disc is dominated by the toroidal component, but the poloidal field becomes comparable when outflow develops. At the disc surface, we typically have $B_{z,r}/B_\phi \simeq 1$. The structure of the poloidal field is shown in Figs. 2(c).

The angle between the disc surface and the field lines is less than 60° in the outer parts of the disc. Thus, the wind is largely magneto-centrifugally driven here: the Alfvén surface is far away from the disc, as can be seen in Fig. 3. However, the thermal pressure gradient is the dominant accelerating force closer to the rotation axis where the flow is well collimated. In fact, the build-up of the pressure gradient near the central object is controlled by our fixed entropy distribution: once the matter leaves the disc, it is heated to a high temperature, which implies enhanced pressure for a given entropy.

Fig. 3 shows that mass replenishment in the disc is concentrated to a few small regions. From these regions, matter accretes inwards and eventually most of it ends up in the collimated outflow.

The collimated, fast, dense part of the outflow has a well defined boundary clearly visible in Fig. 2(a) and (b) and (c). The collimation and confinement is due to the inward pressure gradient produced by the azimuthal field. This can be seen from the right Fig. 2(d) where we show the radial profiles of various pressure components.

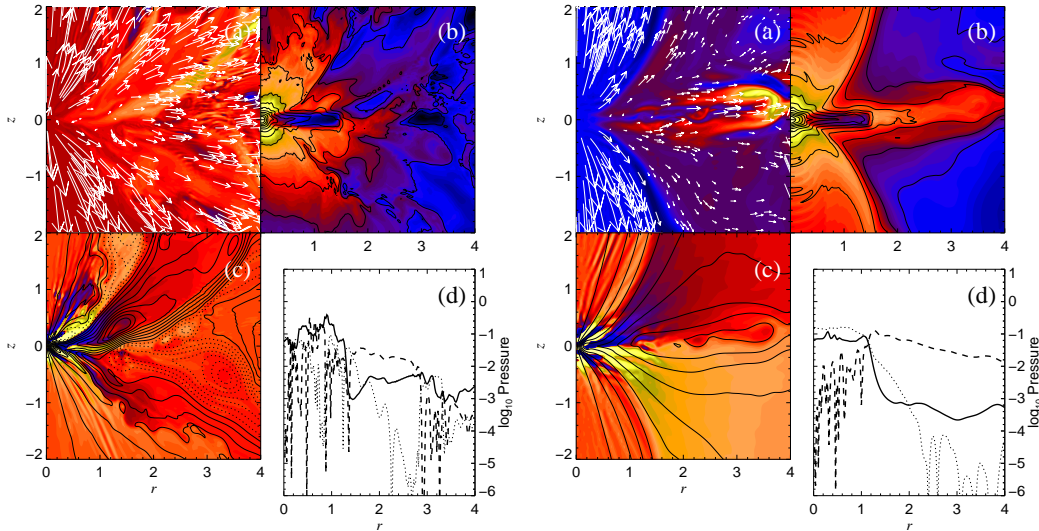


Fig. 2. Overview for $t = 44$ (left) and $t = 88$ (right). (a) Specific angular momentum (colour coded) and poloidal velocity (arrows). (b) Temperature (colour coded) and density (contour lines). (c) Azimuthal (colour coded) and poloidal components (field lines) of magnetic field. (d) Pressure profiles at $z = 1$. Thermal pressure p (solid line); toroidal magnetic pressure (dashed); poloidal magnetic pressure (dotted).

4 Outlook

Our model indicates that a dynamo-generated \mathbf{B} -field can indeed collimate wind from an accretion disc into an axial jet. Many of the idealizations in the model should now be removed to see how far they influence this result.

Particularly, we plan to replace the mass source in the disc by a corresponding inflow through the radial boundary. Further, instead of imposing a fixed entropy profile, we should solve an energy equation, including parameterized heating when matter leaves the disc and radiative cooling, which is expected to be important if the vertical size of the computational domain is $\gtrsim 10$ AU.

On the long term, we plan to extend the model to three spatial dimensions, which will allow us to address, amongst other interesting questions, the problem of MHD stability of the jet.

References

- Blandford, R. D., Payne, D. R. (1982) *MNRAS* **199**, 883.
 Brandenburg, A., Nordlund, Å., Stein, R. F. (1995) *ApJ* **446**, 741.
 Königl, A., Pudritz, R. (1999) in *Protostars and Planets III*, ed. V. Mannings, A. Boss, S. Russell (Univ. Arizona Press) (astro-ph/9903168).
 Kudoh, T., Matsumoto, R., Shibata, K. (1998) *ApJ* **508**, 186.

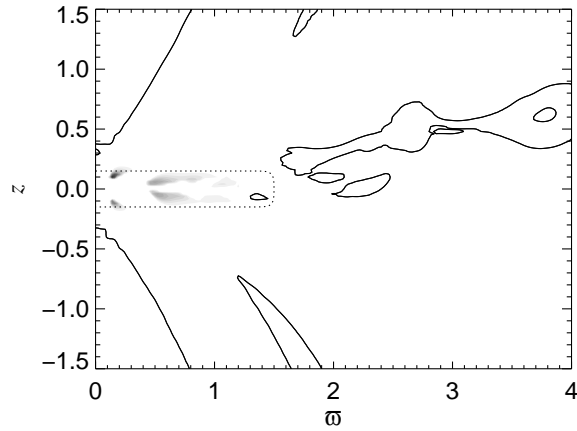


Fig. 3. Alfvén surface (solid line) and local mass production rate q_e (colour coded) in the vicinity of the disc (indicated by the dotted line) at $t = 88$.

- Matsumoto, R., Uchida, Y., Hirose, S., Shibata, K., Hayashi, M.R., Ferrari, A., Bodo, G., Norman, C. (1996) *ApJ* **461**, 115.
- Moss, D., Shukurov, A., Sokoloff, D. (1999), *A&A* **343**, 120.
- Ouyed, R., Pudritz, R. E. (1997a), *ApJ* **482**, 712.
- Ouyed, R., Pudritz, R. E. (1997b), *ApJ* **484**, 794.
- Ouyed, R., Pudritz, R. E. (1999), *MNRAS* (submitted).
- Ouyed, R., Pudritz, R. E., Stone, J. M. (1997), *Nature* **385**, 409.
- Pudritz, R. E. (1981), *MNRAS* **195**, 881.
- Romanova, M. M., Ustyugova, G. V., Koldoba, A. V., Chechetkin, V. M., Lovelace, R. V. E. (1997), *ApJ* **482**, 708.
- Romanova, M. M., Ustyugova, G. V., Koldoba, A. V., Chechetkin, V. M., Lovelace, R. V. E. (1998), *ApJ* **500**, 703.
- Stepinski, T. F.; Levy, E. H. (1988), *ApJ* **331**, 416.
- Stone, J. M., Norman, M. L. (1994), *ApJ* **433**, 746.
- Uchida, Y., Shibata, K. (1985), *PASJ* **37**, 515.
- Urpín, V., Brandenburg, A. (1998), *MNRAS* **294**, 399.
- Ustyugova, G. V., Koldoba, A. V., Romanova, M. M., Chechetkin, V. M., Lovelace, R. V. E. (1995), *ApJ* **439**, L39.